Optimizing Properties of Ultra-low-density Fiberboard *via* Response Surface Methodology and Evaluating the Addition of a Coupling Agent

Zhihui Li, Xinglai Qi, Shiwei Lan, Huibin Wang, Nairong Chen, Junfeng Lin, Ming Lin,* and Jiuping Rao *

The main production process parameters of ultra-low-density fiberboard (UDF) were selected by use of response surface methodology, and then the properties of UDF were improved by adding a coupling agent. Microstructures and chemical bonding in UDF were analyzed by scanning electron microscopy and infrared spectroscopy. The results showed that the desirable process parameters for UDF production were the amount of urea-formaldehyde resin adhesive (18%), the hot pressing temperature (170 °C), the hot pressing time (200 s), and the amount of KH560 coupling agent added (1%). The main physical and mechanical properties of UDF obtained included internal bond strength (0.59 MPa), modulus of rupture (19.8 MPa), and 24h thickness swelling (10.0%). These properties exceeded the requirements of ISO 16895 (2016).

Keywords: Ultra-low-density fiberboard; Response surface methodology; Coupling agent; Chemical bonding

*Contact information: College of Material Engineering, Fujian Agriculture and Forestry University, 350002, Fuzhou, Fujian, China; *Corresponding author: fafurjp@163.com; fjlm403@163.com*

INTRODUCTION

Wood-based panels are widely used in decorations, furniture, vehicles, *etc.*, because of multiple characteristics including low production cost, easy processing, and dimensional stability. The three main types of wood-based panels are plywood, fiberboard, and particleboard. Among these, fiberboard is an important product in the wood industry because it utilizes wood feedstock having a broad range of sizes. Differences in density allow fiberboards to be used for many different applications. Among them, medium density fiberboard (MDF) and high density fiberboard (HDF) were the most widely studied types of boards. Researchers have used response surface methodology to statistically analyze the effects of various hygrothermal post-manufacturing treatments on the physical and mechanical properties of medium-density and high-density fiberboards; it was concluded that this approach can significantly reduce the thickness expansion of the board (Imtiaz *et al.* 2015). In addition, the effects of resin type, resin content, water content and three fiber lengths of kenaf on the physical and mechanical properties of MDF were also studied (Imtiaz *et al.* 2014a,b). However, many applications of MDF and HDF products have excess performance, resulting in a waste of resources. Therefore, it is necessary to develop a low-density fiberboard that can meet the requirements of its desired application (Kawasaki and Kawai 2006; Monteiro *et al.* 2018).

According to ISO 16895 (2016), fiberboards with a density range of 550 $kg \cdot m^{-3}$ to 650 $kg \cdot m^{-3}$ or less than 550 $kg \cdot m^{-3}$ are classified as low-density fiberboard (LDF) and ultra-low-density fiberboard (UDF), respectively. UDF has rapidly developed in recent

years because of its light weight, low density, and porous structure. It is mainly used for non-structural applications, such as sound insulation and thermal insulation (Doosthoseini *et al.* 2010; Niu *et al.* 2014; Cai *et al.* 2016). During the preparation of UDF, there are many advantages when compared with traditional HDF or MDF: (i) more than one third of raw materials can be saved at the same thickness, (ii) manpower and material resources can be saved during processing, production, and transportation, and (iii) the absolute amount of formaldehyde released can be reduced to increase safety for the user and the environment. Traditional UDF is mainly prepared *via* the wet method, which has a complicated operation and produces serious pollution. Although the density is low, the product is more suitable for packaging materials. For example, the liquid foaming method (Xie *et al.* 2011) was used to manufacture UDF in 2011, and the results showed that when the density of the fiberboard was 56.3 $kg.m^{-3}$, the internal bond strength was 0.15 MPa, the modulus of rupture was 0.70 MPa, the modulus of elasticity was 8.91 MPa, and the compressive strength at 10% deformation was 0.17 MPa. The thickness swelling after 24 hours of water immersion (TS) was 0.57%. In addition, researchers have improved the performance of the board by adding other materials. Chen *et al.* studied the effect of different proportions of Si-Al compounds on the microstructure and the mechanical properties of ultra-low density fiberboard (UDF). The results showed that when the Si-Al molar ratio was 2:1, the elastic modulus, rupture of modulus, and internal bond strength of UDF were as high as 20.78, 0.17, and 0.025 MPa, respectively (Chen *et al.* 2016b). For the dry preparation of UDF there are few reports in the literature.

Researchers have studied the hot pressing process of UDF with the single factor test (Niu *et al.* 2018) and the orthogonal test (Yang *et al.* 2014). However, fewer scholars have studied the influence of process parameters on the mechanical properties of UDF by response surface methodology. The objectives of this study are to manufacture ultra-low-density fiberboard via the response surface method and study the effects of various factors on the mechanical properties of these boards, and on this basis further improve the physical and mechanical properties of the board by modifying the adhesive with different proportions of the coupling agent KH560.

EXPERIMENTAL

Materials

Wood fiber was supplied by Furen Group Corporation Co., Ltd. (Fujian, China). The detailed fiber dimensions were approximately 0.8 to 1.2 mm in length and 28 to 30 μm in width. All the fibers were dried to a moisture content of 3.0 to 3.5% and reserved in a sealed plastic container to be used for manufacturing UDF. Urea-formaldehyde resin adhesive (UF) with a solids content of 53% was supplied by Furen Group Corporation Co., Ltd. (Fujian, China). Paraffin wax was supplied by Furen Group Corporation Co, Ltd. (Fujian, China). The silane coupling agent KH560, with an active ingredient content of 97%, was purchased from Jiangsu Chenguang Coupling Co., Ltd. (Jiangsu, China). Chemical grade NH_4Cl with an active ingredient content of no less than 99.5% was purchased from Tianjin Zhiyuan Chemical Reagent Co., Ltd. (Tianjin, China).

Methods

Ultra-low-density fiberboard (UDF) preparation

The fiber was placed into a container and stirred continuously. The UF adhesives, paraffin wax (1% of dried fiber), and NH_4Cl (1% of dried adhesive) were sequentially sprayed into the container and stirred for 5 min. Then the mixture was transferred into a mold for pre-pressing for 5 min to form a mat (350 mm × 350 mm in size). Finally, the mat was hot-pressed in a hot-pressing machine (Dongguan Kesheng Industrial Co., Ltd., Guangdong, China) to obtain UDF with constant thickness. The above procedure was repeated to produce UDF with different parameters (including the amount of UF, hot pressing time and hot pressing temperature) according to a response surface methodology experimental design with a target bulk density of about 510 $kg \cdot m^{-3}$. One-factor pre-experiment was conducted before designing the response surface scheme, and it was concluded that the hot pressing pressure had little effect on UDF, and the hot pressing temperature, hot pressing time and UF addition had a great influence on the performance of UDF.

Based on the desirable conditions of the response surface methodology, the adhesives were physically modified by adding different proportions (0, 0.2, 0.4, 0.6, 0.8, 1.0, and 1.2% of the adhesive) of KH560 to further explore the performance changes of ultra-low-density fiberboard. The specific method was to physically mix the coupling agent KH560 and the UF and then spray it evenly on the surface of the fiber.

Properties evaluation

Prior to the evaluation, the specimens were stored in a conditioning chamber until constant weight was achieved. Modulus of rupture (MOR), internal bond strength (IB) and thickness swelling after 24 hours of water immersion (TS) were tested in accordance with ISO 16895 (2016). The size of specimens for the testing of MOR, IB, and TS were 250 × 50 × 10 mm, 50×50×10 mm, and 50×50×10 mm (L×W×H), respectively. A testing machine (MTS, Shenzhen, China) with a crosshead speed of 5 mm/min was used to test the MOR and IB. The specimens were soaked into a room temperature (25 °C) water bath for 24 h to test the TS. The results are presented as the mean of six replicates (Bao *et al.* 2014; Fernandes *et al.* 2011).

Scanning electron microscopy (SEM) analysis

The fiber was characterized by use of a scanning electron microscope (Nova NanoSEM 230; FEI Company, Tokyo, Japan) to analyze its changes in morphology after different treatments. A small amount of dry wood fiber was treated with a vacuum applicator to coat the surface of the sample with gold (Zeng *et al.* 2018). The sample was then placed on a stage for observation.

Fourier transform infrared (FTIR) spectroscopy analysis

The sample (0.001 g) was uniformly mixed with 0.100 g of KBr, and the chemical bonds of the KH560, UDF, and UDF-KH (UDF prepared by adding KH560 to the UF adhesive) were analyzed by FTIR spectroscopy (American Thermoelectric Corporation, Nicolet 380 FTIR, USA) (Bledzki *et al.* 2010; Chen *et al.* 2015).

RESULTS AND DISCUSSION

Properties of UDF Analysis

UDFs were prepared according to the different parameter combinations, and then the MOR, IB, and TS were evaluated. The results are shown in Table 1.

Table 1. Mechanical and Physical Properties the UDFs

Test Number	(A) UF (%)	(B) Temperature (° C)	(C) time(s)	MOR (MPa)	IB (MPa)	TS (%)
1	16	180	250	14.4	0.51	12.89
2	16	180	250	14.5	0.50	13.17
3	16	170	200	14.4	0.36	13.21
4	16	190	300	13.8	0.37	14.35
5	16	170	300	14.2	0.49	13.51
6	16	180	250	13.7	0.47	13.16
7	14	180	200	12.6	0.42	15.58
8	14	180	300	13.2	0.47	13.88
9	14	170	250	11.7	0.37	14.14
10	16	190	200	13.7	0.47	13.25
11	18	180	200	14.8	0.54	12.46
12	16	180	250	13.8	0.39	14.28
13	16	180	250	13.9	0.41	13.22
14	18	190	250	13.8	0.47	12.85
15	18	180	300	13.2	0.47	13.12
16	18	170	250	14.6	0.59	12.15
17	14	190	250	13.1	0.42	14.65

Design Expert software (Stat-Ease, Inc., Minneapolis, Minnesota) was selected to analyze the coefficients of the parameter variables for the response surface methodology. A quadratic model was used and the following second-order polynomial equations for MOR, IB, and TS were obtained as shown below,

$$MOR = 14.04 + 0.73 \times A - 0.045 \times B - 0.14 \times C - 0.54 \times A \times B - 0.58 \times A \times C + 0.099 \times B \times C - 0.65 \times A^2 - 0.077 \times B^2 + 0.054 \times C^2 \quad (1)$$

$$IB = 0.45 + 0.049 \times A - 0.012 \times B + 0.0009 \times C - 0.040 \times A \times B - 0.030 \times A \times C - 0.059 \times B \times C \quad (2)$$

$$TS = 6.19 - 0.13 \times A + 0.048 \times B - 0.10 \times C \quad (3)$$

where the symbols A, B, and C represent the UF adhesive usage (%), the hot pressing temperature (° C), and the hot pressing time (s), respectively. From Eq. 1, the relative effect of each factor on the MOR was $A > A^2 > AC > AB > C > BC > B^2 > C^2 > B$. From Eq. 2, the relative effect of each factor on the intensity of static bending was $BC > A > AB > AC > B > C$. From Eq. 3 it can be concluded that the relative effect of each factor on the 24 h water absorption thickness expansion was $A > C > B$. The variance analyses of MOR, IB, and TS carried out by the Design Expert software are displayed in Table 3, Table 4, and Table 5, respectively.

Table 2 shows that the p-value of the model was 0.0197, which is less than 0.05, indicating that the model was significant, the fitting accuracy was good, and the response surface approximation model can be used to choose desirable conditions. Among the effects listed, the p-value for A was 0.002, which is less than 0.01, indicating that the amount of UF had a significant effect on the MOR. The p-values for AB AC and A^2 were 0.0399, 0.0312, and 0.0171, respectively. These were all less than 0.05, indicating that the interaction of the amount of UF and hot pressing temperature, the interaction of the amount of UF and hot pressing time, and the square of the amount of UF had significant effects on the MOR. The results of the variance analysis of the regression equations show the lack of fit had a p-value of 0.3296＞0.05, which indicates that the equation fit well to the test results with small error. Therefore, the regression equation can be used to determine the desirable process conditions.

Table 2. Analysis of Variance of MOR

Source	Sum of Squares	Degrees of Freedom (DF)	Mean Square	F Value	P-value Prob＞F	
Model	8.8172	9	0.9797	5.2718	0.0197	Significant
A	4.2249	1	4.2249	22.7347	0.0020	
B	0.0165	1	0.0165	0.0887	0.7745	
C	0.1675	1	0.1675	0.9012	0.3741	
AB	1.1792	1	1.1792	6.3456	0.0399	
AC	1.3424	1	1.3424	7.2237	0.0312	
BC	0.0391	1	0.0391	0.2104	0.6604	
A^2	1.7946	1	1.7946	9.6569	0.0171	
B^2	0.0248	1	0.0248	0.1337	0.7254	
C^2	0.0125	1	0.0125	0.0672	0.8029	
Residual	1.3008	7	0.1858			
Lack of Fit	0.7022	3	0.2341	1.5639	0.3296	Not Significant
Pure Error	0.5986	4	0.1497			
Corrected Total	10.1180	19				

Note: Prob＞F is the probability of no significant influence. A value less than 0.05, is significant.

Table 3 shows that the model p-value was 0.0431, which is less than 0.05, indicating that the model is significant and the fitting accuracy is good. Among the effects listed the p-value for A was 0.0143, which is less than 0.05, indicating that the amount of UF had a significant effect on the IB. The p-value for BC is 0.0294＜0.05, indicating that the interaction between hot press time and hot press temperature had a significant effect on the IB. From the results of the variance analysis of the regression equations, it can be seen that the lack of fit had a p-value of 0.7396, which is greater than 0.05, which indicates that the error between the equation and the test results was not significant, so the fitting of IB was very good.

Table 3. Analysis of Variance of IB

Source	Sum of Squares	DF	Mean Square	F Value	P-value Prob＞F	
Model	0.0438	6	0.0073	3.3914	0.0431	Significant
A	0.0189	1	0.0189	8.7603	0.0143	
B	0.0011	1	0.0011	0.4934	0.4984	
C	0.0000	1	0.0000	0.0030	0.9573	
AB	0.0065	1	0.0065	3.0101	0.1134	
AC	0.0035	1	0.0035	1.6374	0.2296	
BC	0.0139	1	0.0139	6.4439	0.0294	
Residual	0.0215	10	0.0022			
Lack of Fit	0.0100	6	0.0017	0.5770	0.7396	Not Significant
Pure Error	0.0115	4	0.0029			
Corrected Total	0.0654	16				

Table 4 shows that the p-value of the model was 0.0019, which is less than 0.05, indicating that the model was significant and the fitting accuracy was good. The response surface approximation model can be used to choose desirable conditions. Among the effects listed, the p-value for A was 0.0003, which is less than 0.01, indicating that the amount of UF had a significant effect on the 24 h water absorption thickness expansion. The variance analysis of the regression equations show that the missing term of the equation had a p-value of 0.5269, which indicates that the error between the equation and the test results was not significant, so the fitting of TS was very good.

Table 4. Analysis of Variance of TS

Source	Sum of Squares	DF	Mean Square	F Value	P-value Prob＞F	
Model	7.9050	3	2.6350	8.7830	0.0019	Significant
A	7.3489	1	7.3489	24.4953	0.0003	
B	0.5403	1	0.5403	1.8008	0.2026	
C	0.0159	1	0.0159	0.0529	0.8216	
Residual	3.9002	13	0.3000			
Lack of Fit	2.7320	9	0.3036	1.0395	0.5269	Not Significant
Pure Error	1.1681	4	0.2920			
Corrected Total	11.8052	16				

Desirable conditions of the Preparation Process of Fiberboard

The preparation process of fiberboard was selected using the Design Expert software. The desirable condition was as follows: the amount of resin binder was 18%, the hot pressing time was 200 s, and the hot pressing temperature was 170 °C. In order to prove the reliability of results from the Design Expert software, it is necessary to repeat the test with the desirable process conditions, the results are given in Fig. 1.

Figure 1 shows that the predicted values of IB, MOR, and TS were 0.52 MPa, 15.5 MPa, and 12.3%, respectively. The actual measured values were 0.57 MPa for IB, 15.7 MPa for MOR, and 13.2% for TS. Compared with the predictive values, the IB and MOR were increased by 9.6% and 1.3%, respectively. This indicates that the Box-Behnken design scheme is reliable for the selection of desirable conditions for UDF production.

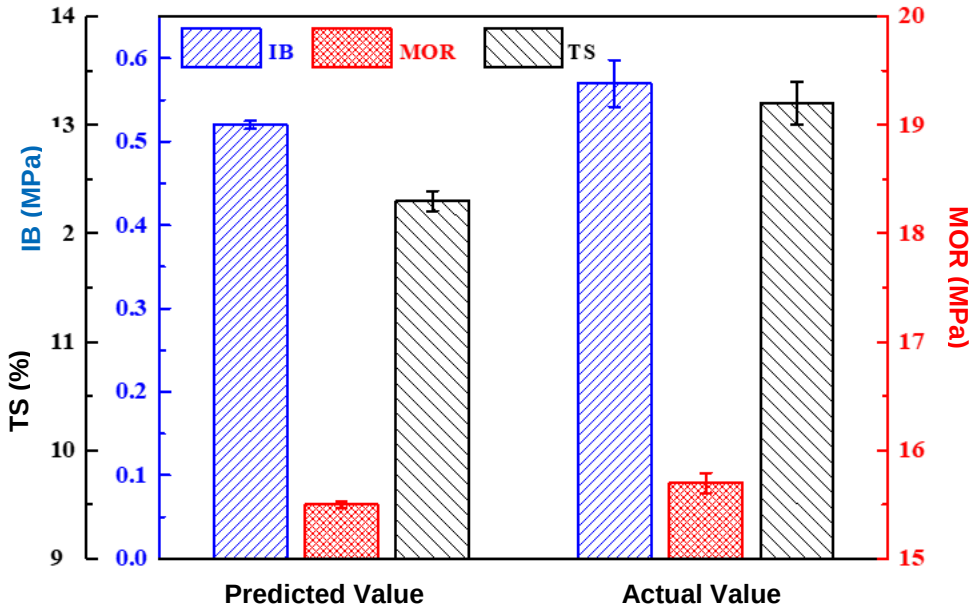

Fig. 1. Predicted and actual values of mechanical properties

UDF Properties Improvement

The properties of the UDF prepared *via* the desirable conditions could not meet the requirements of ISO 16895 (2016). To further improve the properties of UDF, the interface of UF adhesive and fiber was modified by the coupling agent KH560. The results are given in Fig. 2.

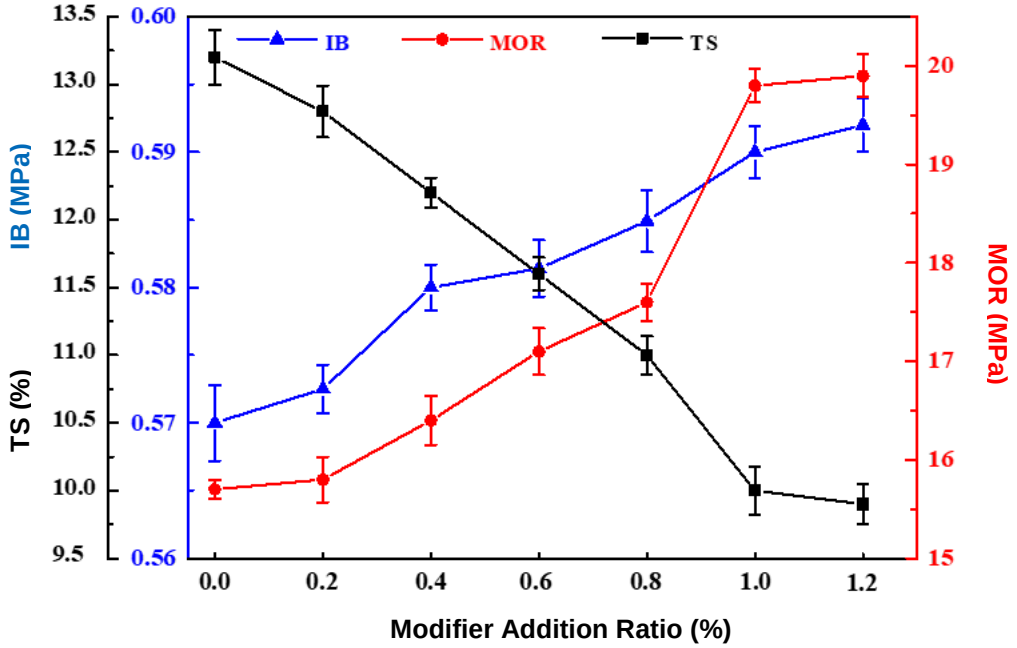

Fig. 2. Mechanical properties after modification of adhesive

As shown in Fig. 2, MOR and IB increased as the amount of KH560 usage increased, whereas the reverse occurred for TS. The reason was that the coupling agent was added to improve the ductility of the adhesive, so that the IB of the UDF was significantly improved, and it was difficult for water to enter the UDF, thereby reducing the thickness expansion of the UDF. The increase of MOR could be observed with 1% of KH560. A similar tendency was also found in the IB. The MOR, IB, and TS of the UDF were 19.8 MPa, 0.59 MPa, and 10.0%, respectively, which met the requirements of ISO 16895 (2016).

Micromorphology of Fiber

To investigate the differences in the pure wood fiber, wood fiber with adhesive, and wood fiber with coupling agent and adhesive, the SEM results were analyzed (Fig. 3).

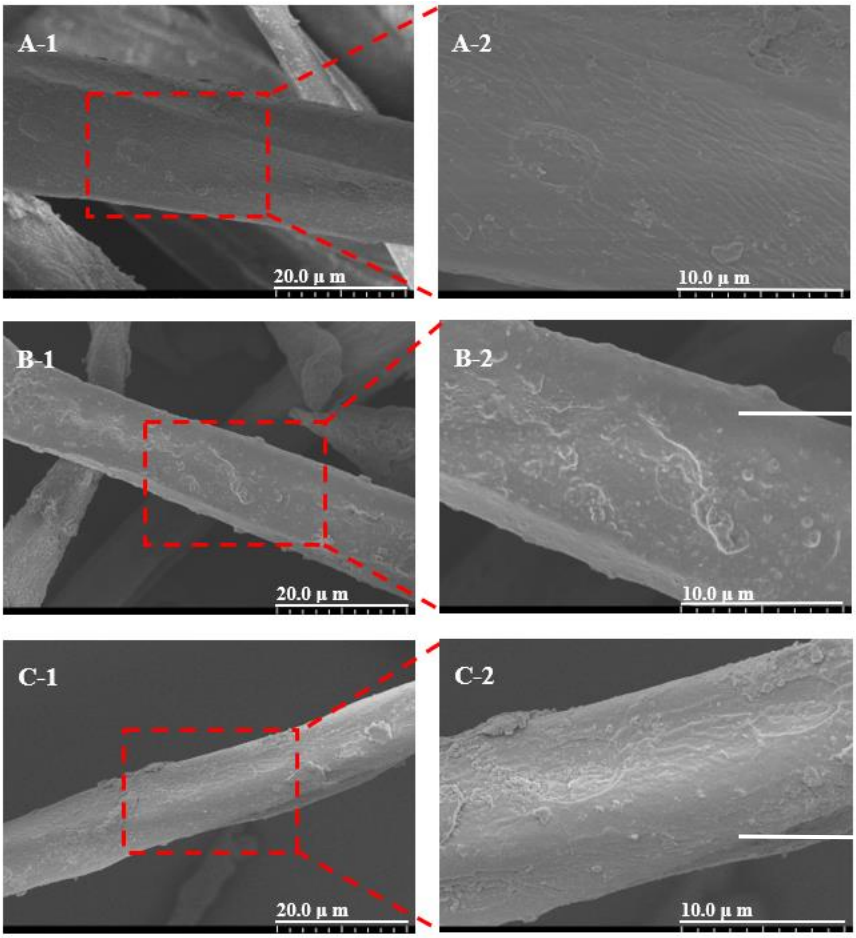

Fig. 3. Microscopic morphology of fibers by different treatment methods

It can be seen that the surface of the pure wood fiber (A-1 and A-2) was relatively smooth, and the angle of the fines of the fiber can be clearly seen to be 10° to 20° from the direction of the fiber. After adhesive was added, the surface of the fiber (B-1 and B-2) was rough and there was a bright material with an irregular shape. The fines of the fiber were not visible, indicating that the adhesive had been uniformly covered onto the surface of the fiber and could bond well to improve the IB of the UDF. However, compared to B-

1 and B-2, the fiber surface of C-1 and C-2 was smoother after the addition of the coupling agent. This was because KH560 increased the surface tension of the fiber and facilitated the resin to spread on the fiber surface. In addition, KH560 is plastic at the interface and can form a flexible deformation layer at the interface; this deformation layer has ability to heal automatically when it is damaged, it is beneficial to prevent the expansion of the crack on the board surface. It is helpful to improve the bond strength between fibers and reduce the thickness expansion of the sample (Ye *et al.* 2007; Liang *et al.* 2012; Liu *et al.* 2012).

FTIR Analysis

To further understand the reaction between cured UF adhesive and fiber, FTIR spectroscopy was performed. Figure 4 shows the FTIR spectra of KH560, UDF with KH560, and UDF without KH 560.

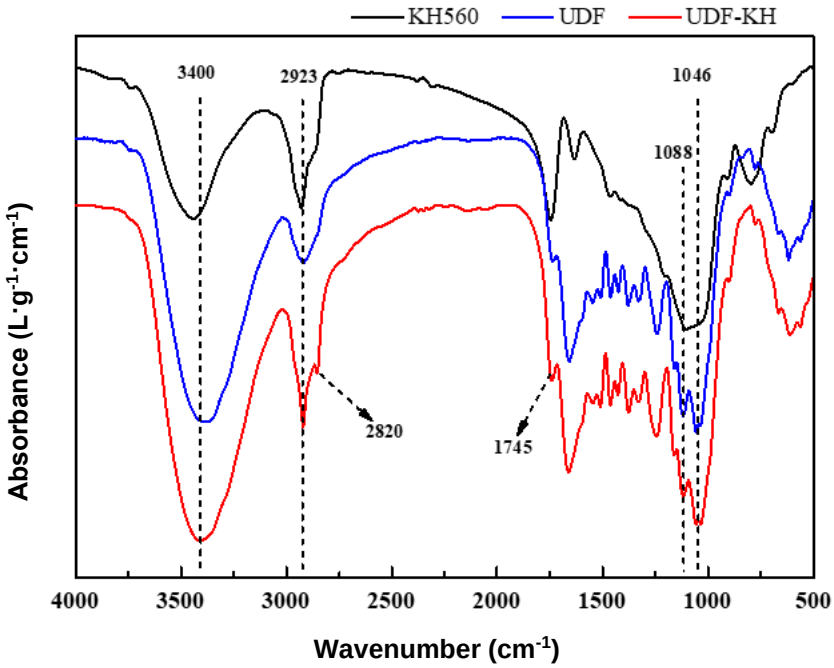

Fig. 4. FTIR spectra of KH560, UDF, and UDF-KH

The FTIR spectra of the coupling agent is represented as KH560, the UDF prepared by adding KH560 to the UF adhesive is represented by UDF-KH, and the UDF without coupling agent added is represented by UDF. The spectra were shown in Fig. 4. It can be seen that the characteristic peak change of O-H at 3400 cm^{-1} was not obvious, it indicated that there were a large number of hydroxyl groups in the fiberboard before and after the treatment of the KH560 (Wu *et al.* 2013). For the unmodified sample, it can be seen that the characteristic vibration peak at about 2923 cm^{-1}(C-H) and 1745 cm^{-1} (C=O) were weak. For the modified sample, a new characteristic peak appeared in 2820 cm^{-1}, it can be concluded that the generation of saturated C-H. In addition, the C-O-C at 1088 cm^{-1} was weakened after the addition of the coupling agent KH560, while the Si-O-Si peak at 1046 cm^{-1} was enhanced (Mai *et al.* 2017; Zhuang *et al.* 2018). In conclusion, the appearance and enhancement of some characteristic peaks indicated the possibility of a grafting reaction of KH560, UF adhesive, and wood fiber during hot pressing which improved the properties of UDF (Chen *et al.*2016(a); You *et al.* 2017; Rao *et al.* 2018).

CONCLUSIONS

1. The desirable parameters for preparing UDF were achieved with a UF adhesive addition of 18%, a hot pressing temperature of 170 °C, and a hot pressing time of 200 s. The corresponding properties of the UDF were 0.57 MPa, 15.7 MPa, and 13.2% for IB, MOR, and TS, respectively. The Box-Behnken design scheme is reliable for the selection of desirable conditions for UDF production.
2. The KH560 used as a coupling agent has an important influence on the properties of UDF. When 1% of KH560 was added, the MOR, IB, and TS of the UDF were 19.8 MPa, 0.59 MPa, and 10.0%, respectively, which met the requirements of ISO 16895 (2016).

ACKNOWLEDGEMENTS

The authors are grateful for the financial supports of the Science & Technology Program in Fujian Province of China (2017N3009) and the Science & Technology Innovation Program in Fujian Agriculture and Forestry University of China (CXZX2017375).

REFERENCE CITED

Bledzki, A. K., Mamun, A. A., and Volk, J. (2010). "Barley husk and coconut shell reinforced polypropylene composites: The effect of fibre physical, chemical and surface properties," *Composites Science and Technology* 70(5), 840-846. DOI: 10.1016/j.compscitech.2010.01.022

Cai, L. L., Zhuang, B. R., Huang, D. B., Wang, W., Niu, M., Xie, Y. Q., Chen, T. J., and Wang, X. D. (2016). "Ultra-low density fibreboard with improved fire retardance and thermal stability using a novel fire-resistant adhesive," *BioResources* 11(2), 5215-5229. DOI: 10.15376/biores.11.2.5215-5229

Chen, B., Shi, Y. F., Xue, Q. S., Lv, J., Shen, D. Y., Wang, Q. L., and Xing, X. Q. (2016a). "Preparation of Antireflective coating on Resin lenses surface and research the capability," *Science and Technology Innovation Herald* 13(27):67-68. DOI: 10.16660/j.cnki.1674-098x.2016.27.067

Chen, T. J, Wu, Z. Z, Niu, M., Xie, Y. Q., and Wang, X. D. (2016b). "Effect of Si–Al molar ratio on microstructure and mechanical properties of ultra-low density fiberboard," *European Journal of Wood & Wood Products* 74(2), 151-160. DOI: 10.1007/s00107-015-0986-x

Chen, Y. G., Li, X., Zhao, H. X., Wang, C. H., Zhang, W. Y., and Shi, Y. G. (2015). "Influence of silane coupling agent on interface interaction and properties of nano-silica/silicone rubber composites," *China Synthetic Rubber Industry* 38(3), 200-205. DOI: 10.3969/j.issn.1000-1255.2015.03.008

Doosthoseini, K., Zarea-Hosseinabadi, H., and Moradpour, P. (2010). "Low resin medium density fiberboard made from chemical activated hardwoods fibers," *Journal of the Indian Academy of Wood Science* 7(1-2), 36-42. DOI: 10.1007/s13196-011-0008-5

Fernandes, E. M., Correlo, V. M., Chagas, J. A. M., Mano, J. F., and Reis, R. L. (2011). "Properties of new cork–polymer composites: Advantages and drawbacks as compared with commercially available fibreboard materials," *Composite Structures* 93(12), 3120-3129. DOI: 10.1016/j.compstruct.2011.06.020

Imtiaz, A., K, Jayaraman., and D, Bhattacharyya. (2014a). "Implications of fiber characteristics and mat densification on permeability, compaction and properties of kenaf fiber panels, " *Industrial Crops and Products* 61, 293-302. DOI: 10.1016/j.indcrop.2014.07.018

Imtiaz, A., Jayaraman, K., and Bhattacharyya, D. (2014b). "Effects of resin and moisture content on the properties of medium density fibreboards made from kenaf bast fibres," *Industrial Crops and Products* 52, 191-198. DOI: 10.1016/j.indcrop.2013.10.013

Imtiaz, A., Jayaraman, K., and Bhattacharyya, D. (2015). "Dimensional stability improvement of kenaf panels by post-manufacturing hygrothermal treatments using response surface methodology," *Industrial Crops and Products* 67, 422-431. DOI: 10.1016/j.indcrop.2015.01.071

ISO 16895 (2016). "Wood-based panels — Dry-process fibreboard, "International Organization for Standardization, Geneva, Switzerland.

Kawasaki, T., and Kawai, S. (2006). "Thermal insulation properties of wood-based sandwich panel for use as structural insulated walls and floors," *Journal of Wood Science* 52(1), 75-83. DOI: 10.1007/s10086-005-0720-0

Liang, C., Zhan, H. Y., Qin, C. R., Lv, J., Shen, D. Y., Wang, Q. L., and Xing, X. Q. (2012). "SEM-EDS Analysis of fiber surface of sulfonated chemimechanical pulps," *Paper Science & Technology* 31(6), 110-114. DOI: 10.19696/j.issn1671-4571.2012.06.027

Liu, J., Qiu, Y., Wang, J., Xiang, H. Y., Xu, R. F., Li, J., Li, Q. H., and Xu, A. C. (2012). "Studies on fiber morphologies of domestic and imported paper-process reconstituted tobacco, "*China Pulp Paper Industry* (16), 10-13. DOI: 10.3969/j.issn.1007-9211.2012.16.002

Mai, C., Direske, M., Varel, D., and Weber, A. (2017). "Light medium-density fibreboards (MDFs): does acetylation improve the physico-mechanical properties?," *European Journal of Wood and Wood Products* 75(5), 739-745. DOI: 10.1007/s00107-016-1147-6

Monteiro, S., Martins, J., Magalhães, F. D., and Carvalho, L. (2018). "Lightweight wood composites: Challenges, production and performance," *Lignocellulosic Composite Materials* 293-322. DOI: 10.1007/978-3-319-68696-7_7

Niu, M., Hagman, O., Wang, A., Xie, Y. Q., Karlsson, O., and Cai, L. L. (2014). "Effect of Si-Al compounds on fire properties of ultra-low density fiberboard," *BioResources* 9(2), 2415-2430. DOI: 10.15376/biores.9.2.2415-2430

Niu, M., Wu, Z. Z, Lin, X. Q., Liu, Z. Q., Xie, Y. Q., and Wang, X. D. (2018). "Manufacturing and properties of ultra-low density fiberboards with an unsaturated polyester resin by a dry process," *European Journal of Wood and Wood Products* 76(3), 853-859. DOI: 10.1007/s00107-017-1252-1

Rao, J. P., Bao. L. X., Wang, B. W., Fan. M. Z., and Feo, L. (2018). "Plasma surface modification and bonding enhancement for bamboo composites," *Composites Part B: Engineering* 138, 157-167. DOI: 10.1016/j.compositesb.2017.11.025

Wu, Y. K., and Zhang, G, L., (2013). "Crystallinity and Fourier transform infrared spectroscopy analysis of the modified sunflower stalk," *Journal of Northwest*

Forestry 28(05), 172-174. DOI: 10.3969/j.issn.1001-7461.2013.05.34

Xie, Y. Q., Tong, Q. J., Chen, Y., Liu, J. H., and Lin, M. (2011). "Manufacture and properties of ultra-low density fibreboard from wood fibre," *BioResources* 6(4), 4055-4066. DOI: 10.15376/biores.6.4.4055-4066

Yang, Y. F., Ye, X. Q., and Chen, Z. G. (2014). "Hot pressing process of high-performance low density fiberboard," *China Wood-Based Panels* (6), 8-10. DOI: 10.3969/j.issn.1673-5064.2014.06.003

Ye, X. P., Julson, J., Kuo, M., Womac, A., and Myers, D. (2007). "Properties of medium density fiberboards made from renewable biomass," *Bioresource Technology* 98(5), 1077-1084. DOI:10.1016/j.biortech.2006.04.022

You, S. Y., Dai, R. Y., Dong, X. N., Li, L., Chen, Y. H., and Cao, X. (2017). "Synthesis and properties of phenolic resin modified by silane coupling agent," *China Synthetic Resin and Plastics* 34(06):17-19.

Zeng, Q. Z., Lu, Q. F., Zhou, Y, Z., Chen, N. R., Rao, J. P., and Fan, M. Z. (2018). "Circular development of recycled natural fibers from medium density fiberboard wastes," *Journal of Cleaner Production* 202, 456-464. DOI: 10.1016/j.jclepro.2018.08.166

Zhuang, B. R., Zhan, Y. P., Huang, W. Y., Ye, H. L., and Xie, Y. Q. (2018). "Smoke suppression properties of Si-Al mesoporous structure on medium density fiberboard," *Journal of Hazardous Materials* 357(5), 271-278. DOI: 10.1016/j.jhazmat.2018.05.068

Article submitted: January 22, 2019; Peer review completed: March 23, 2019; Revised version received: April 1, 2019; Accepted: April 5, 2019; Published: April 17, 2019.
DOI: 10.15376/biores.14.2.4373-4384